Perfluorocarbons and their use in Cooling Systems for Semiconductor Particle Detectors

V. Vacek[1,3*], G. Hallewell[2,3], S. Ilie[3] and S. Lindsay[4].

[1]*Czech Technical University, Prague, Czech Republic;*
[2]*Centre de Physique des Particules de Marseille, France;*
[3]*CERN, 1211Geneva 23, Switzerland*
[4] *Department of Physics, University of Melbourne, Australia*

Abstract

We report on the development of evaporative fluorocarbon cooling for the semiconductor pixel and micro-strip sensors of inner tracking detector of the ATLAS experiment at the future CERN **L**arge **H**adron **C**ollider (LHC). We proceeded with studies using perfluoro-n-propane (3M-"PFG $_3F_8$), perfluoro-n-butane (3M-"PFG 5040"; C_4F_{10}), trifluoro-iodo-methane (CF_3I) and custom C_3F_8/C_4F_{10} mixtures. Certain thermo-physical properties had to be verified for these fluids. Sound velocity was calculated for the pure fluids and custom mixtures. A Sonar instrument was developed for the measurement of sound velocity in the above fluids at a variety of temperatures and pressures. Irradiation studies were made on the fluids using neutrons and gamma rays to determine their suitability for use in the high radiation environment at LHC.

Keywords: Data, experimental method, velocity of sound, alternative refrigerants, perfluoro-carbons, mixtures.

---

1. Introduction

The silicon substrates of the silicon pixel and micro-strip sensors of the ATLAS inner tracker [1, 2] must be continuously operated at a temperature below –7ºC for a ~ 10 year operational lifetime at LHC. In addition, for physics motivations, the detector cooling system must present the minimum possible extra material. We have therefore investigated evaporative cooling with the fluorinated hydrocarbons of Table 1. These combine high heat transfer coefficients with very low circulating coolant mass (1–2 g s^{-1}/100W to evacuate). Liquid refrigerant can be delivered to the detector in capillaries with IDs as small as 0.6 mm or via ruby injectors. Other attractive features of fluorocarbon fluids in our application include high dielectric constant, non-flammability and high expected radiation resistance. The high radiation environment does, however, constrain the cooling circuits to operate in an oil-free mode this makes their design rather difficult.

* Corresponding Author

The pixel and micro-strip detectors are divided into around 320 linear and disk-like arrays of silicon sensor tiles. The linear arrays ("ladders") have lengths varying between 80 and 160 cm with up to 13 sensors tiled along them. Individual sensors dissipate a maximum of ~10 Watts, and cooling measurements were made up to the full projected power with heat transfer to the evaporative coolant through an area ranging between 3.5 and 12 cm^2. The total dissipation of the ATLAS semiconductor tracking detectors will be around 60kW, and the final cooling system will comprise around 400 parallel evaporative channels with individual control of flow rate and evaporating temperature, supplied from a central compressor station.

Latent heat data for the various refrigerants are shown in Table 1, together with their saturated vapor pressures and the volume (cm^3) of vapor produced per cm^3 liquid evaporated at –15ºC (a temperature chosen to accommodate probable thermal impedances between the silicon substrates and the coolant). A target evaporation pressure of 1 bar_{abs} would allow the use of very low-mass tube (~0.2 mm wall aluminum or composite) in a variety of aspect ratios.

Table 1
Selected Refrigerant Properties (-15º C)

Fluid formula	Latent heat [$kJ\ kg^{-1}$]	Liquid-Gas Expansion Factor	S.V.P. at -15º C [bar_{abs}]
C_3F_8	97	71.4	2.46
C_4F_{10}	101.1	242.6	0.58
CF_3I	100.8	176.3	1.33
C_3F_8/C_4F_{10} (50/50, molar)	98.3	147.6	$1.01P_{SV} - 1.65\ P_{SL}$

For the design of an effective cooling system [3], most of the engineering design parameters had to be studied. Presented results from the studies include:

- verification of fluid behavior reflecting predictions of the thermodynamic and transport properties of fluids [4, 5, 6] - the cooling circuit of Fig. 1 was used for this purpose and several pilot detector structures were tested;

- velocity of sound measurements at low pressures [up to 4 bar_{abs}], performed mainly to verify the thermodynamic property predictions for the fluids, and to determine the composition of custom binary mixtures;

- heat transfer coefficient measurements during evaporation [6] for various heat fluxes (powers) and different fluids and mixtures;

- effects of neutron and gamma ray irradiation upon the fluids of interest.

2 Measurement Apparatus

2.1. The Evaporative Recirculator

A closed-loop evaporative recirculator (Fig. 1) has been built for testing thermo-structures using all the fluids of Table 1. Structures are placed in a chamber purged with an inert gas (N_2) and maintained at –7ºC, to simulate the environment of the silicon sensors in ATLAS.

The present circulator contains two compressor stages and a water-cooled condenser, also serving as a high-pressure liquid refrigerant reservoir. The first stage compressor[1] is used only with low input pressure vapors as in the case of C_4F_{10}, CF_3I or C_3F_8/C_4F_{10}, since the pumping speed of the second stage compressor[2] is insufficient at input pressures below 1 bar_{abs}. This complexity was required to test four thermodynamically different fluids. These compressors will soon be replaced with a single stage dry scroll compressor[3], with a measured pumping speed of ~20 m^3hr^{-1} for both C_4F_{10} (P_{in} = 0.25, P_{out} = 4 bar_{abs}) and C_3F_8 (P_{in} = 1.4, P_{out} = 8 bar_{abs}).

Liquid refrigerant enters a four-channel supply manifold, whose pressure - defined by a regulator – determines the liquid mass flow. Fluid enters the test structures via capillaries with diameters varying between 0.6 and 1 mm, or via injectors made from synthetic ruby watch bearings with orifices varying between 210 and 300 µm. The temperature of evaporation of fluid in the test structures depends on the pressure in a 4-channel vapor collection manifold tank, controlled via feedback from a pressure sensor[4] to a variable orifice valve located between the tank and the compressor input. The circulating mass flow is metered after the tank.

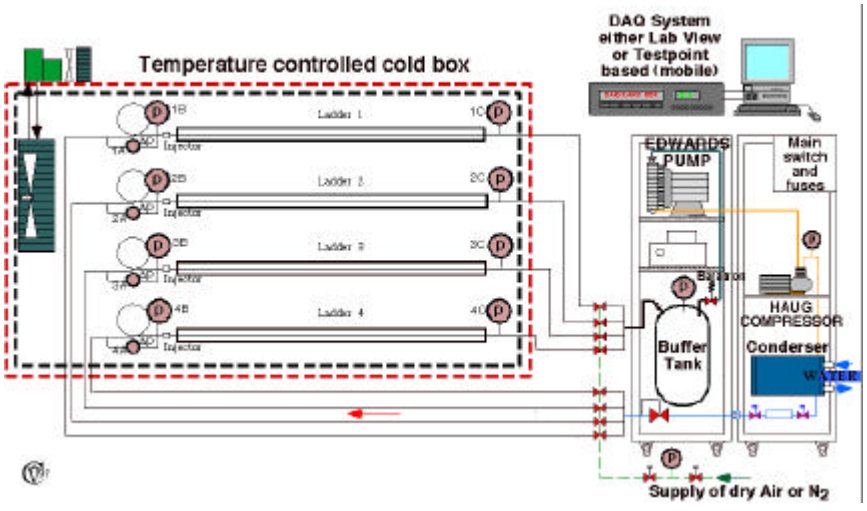

Fig. 1. The Two-Stage Evaporative Recirculator

[1] Edwards ECP 30 Dry Rotary Scroll Vacuum pump (rated 30 m^3hr^{-1} air; P_{in} 1 bar_{abs}, P_{out} = 1.5 bar_{abs} limit)

[2] Haug SOGX 50-D4 Dry Piston Compressor (rated 3.6 m^3hr^{-1} air, P_{in} 1 bar_{abs}; P_{out} = 9 bar_{abs} limit)

[3] Atlas Copco Type SF4-8-120

[4] MKS Baratron Model 122B Range 0-5000 $Torr_{abs}$

2.2. The Sonar Gas Analyzer

There were two main reasons for preparing the sonar gas analyzer:

- to verify available thermodynamic data for fluids of interest;
- to make a fast purity check of delivered fluids, and for possible verification of mixture compositions.

The sonar gas analyzer is shown in Fig. 2a. An aluminum tube contains a pair of ultrasonic transducers[5] having a peak response at 45kHz, and a separation of 944.5 ± 1.0 mm. The tube is surrounded by a coiled copper tube through which coolant was circulated over a temperature range from –20° to 40° C. The temperature of the vapor within the tube was sampled to a precision ± 0.1 °C by of pair of calibrated PT100 sensors. Pressure was monitored to ± 1 torr by an electronic pressure gauge[6].

The timing sequence is shown in Fig 2b., and is based on an earlier development [7]. Packets of eight 45 kHz sound cycles are generated and transmitted through the vapor in the tube. Synchronous with the leading edge of the first cycle (A), a fast (4 MHz) transit time clock is started. This clock is stopped when an above-threshold sound signal is received (B), and the number of counted pulses is used together with the path length to calculate the sound velocity.

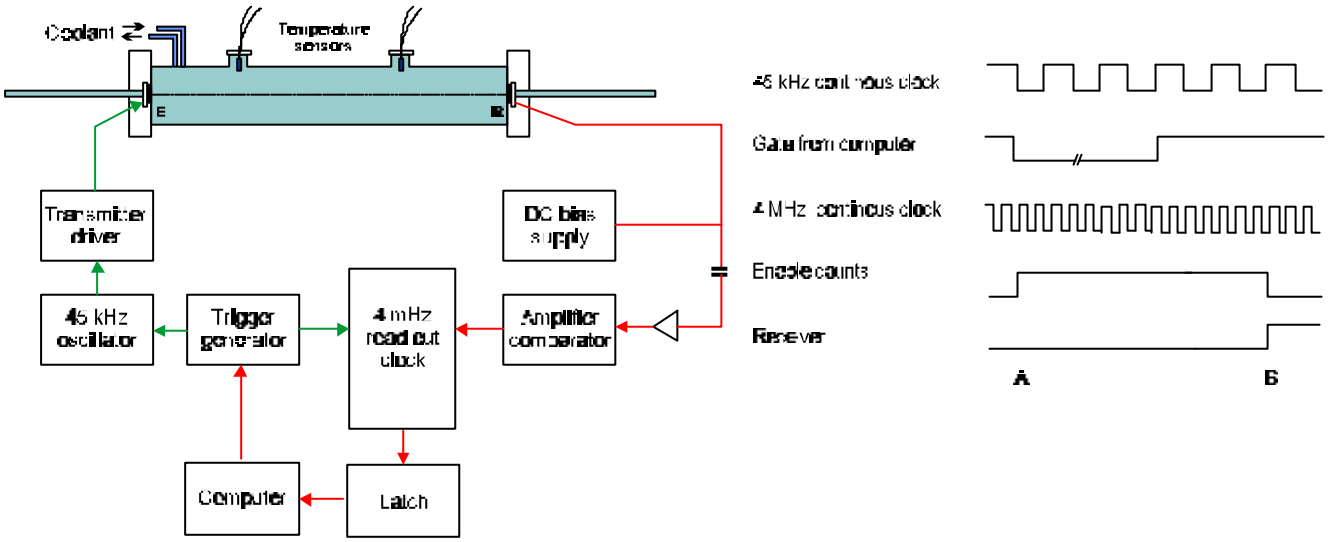

2a. View of the sonar gas analyzer. 2b. Timing Sequence of the sonar

Fig. 2. Schematics of the Sonar analyzer

[5] Polaroid Corp. Instrument grade transducer, part no 604142

[6] MKS Corp. "Baratron" Model 122B read by MKS Corp. Model 600 Pressure Controller.

2.3. Apparatus for Heat Transfer Coefficient (HTC) Measurements

A second small, dry refrigeration circuit was constructed to allow simultaneous measurements of heat transfer coefficient (HTC) while full size thermo-structure prototypes were measured in the main circulator. Heat transfer coefficients were measured on a simplified "ladder" having 12 copper blocks soft-soldered onto a 1.6 m long cupro-nickel tube with 3.6 mm ID. On each block were a ceramic heater and a PT100 sensor. PT100's were fitted to the coolant tube in 13 positions between the blocks and at each end. Another sensor measured the liquid temperature upstream of the capillary or injector. In this tube, HTCs were deduced at 12 points along the tube from the (*block-tube*) temperature difference, and knowledge of the dissipation at each block and its contact area with the tube.

3. Experimental Results

3.1. Overall performance of the cooling set up with different fluids

Satisfactory cooling of most of the thermal prototypes of the ATLAS silicon micro strip and pixel detectors was demonstrated and has been reported in detail elsewhere [8]. Tests were made up to the full power dissipation (section 1.). The low boiling pressure (0.350 bar_{abs} at ~ –25ºC) and high vapor expansion volume of C_4F_{10} return a relatively high volume of vapor at low pressure at the input of the compressor. The temperature gradient (T_{in}-T_{out}) seen on structures tested with C_4F_{10} was considerably larger than those seen with the other fluids at the same power, indicating that a larger hydraulic diameter would be needed with C_4F_{10} to compensate for the correspondingly higher pressure drop.

3.2. Sonar tests results

The sonar analyzer was calibrated with a range of gases before being used with the various refrigerants. The theoretical value of sound velocity, v_t, for an ideal gas is given by:

$$v_t = \sqrt{\frac{k\ RT}{m}}\ , \qquad (1)$$

where k is the ratio of specific heats, R is the universal gas constant, T the absolute temperature and m the molar mass.

In nitrogen {helium} at 21.0ºC the measured velocities were 349.7 {996.1} ms^{-1}: around 0.3% {0.2%} lower than the ideal gas predictions of 350.6 {998.0} ms^{-1}. The most useful calibration gas was xenon, which combines near ideal behavior with a molar mass (131.3g) closest to those of the heavy refrigerants. Table 2 compares velocity measurements in xenon over a range of temperatures with ideal gas predictions.

Table 2
Velocity of Sound in Xenon

T_{tube}	P_{abs}	SOS	Theor. SOS	DIFF=M.-Th.	Rel._Err.
[C]	[MPa_{abs}]	[ms^{-1}]	[ms^{-1}]	[ms^{-1}]	[-]
-5.5	0.095	166.72	167.73	-1.010	-0.0061
0	0.107	169.22	169.44	-0.224	-0.0013
2.9	0.098	169.71	170.34	-0.632	-0.0037
11.5	0.102	172.73	172.96	-0.232	-0.0013
19.3	0.108	175.67	175.34	0.330	0.0019
20.8	0.107	176.38	175.77	0.614	0.0035
27.8	0.109	178.78	177.86	0.922	0.0052

The first test on a refrigerant was made with R404A[7], for which sound velocities are predicted in the standard NIST REFPROP package [4] according to a modified Benedict-Webb-Rubin equation of state. Our results are summarized in Table 3, and differ by an average relative error of - 0.3% from the NIST predictions at temperatures above 0°C, and by -1.2% for data below -10°C. The observed discrepancy might be explained by a small amount of impurities in the sample (~1%) as seen in gas chromatography of the fluid.

Table 3
Velocity of Sound in R404A

	Temperature											
	-19.45		**-10**		**0**		**10**		**20**		**28**	
P_abs	SOS	STDV	SOS	STDV	SOS	STDV	SOS	STDV	SOS	STDV	SOS	STDV
[MPa]	[ms^{-1}]	[-]	[ms^{-1}]	[-]	[ms^{-1}]	[-]	[ms^{-1}]	[-]	[ms^{-1}]	[-]	[ms^{-1}]	[-]
0.010	154.29	0.11	150.75	0.55	159.74	0.05	162.60	0.11	165.62	0.14	167.75	0.65
0.020	152.21	0.30	155.41	0.20	159.56	0.15	162.57	0.14	165.60	0.50	167.60	0.36
0.030	152.15	0.20	155.24	0.10	159.44	0.15	162.48	0.13	164.90	0.40	167.56	0.17
0.050	151.75	0.10	154.94	0.15	159.14	0.12	162.25	0.13	164.70	0.15	167.40	0.20
0.070	151.26	0.16	154.72	0.18	158.35	0.10	131.70	0.13	164.38	0.14	166.92	0.19
0.100	150.35	0.16	153.96	0.14	157.85	0.10	161.10	0.11	163.92	0.14	166.48	0.18
0.150	148.92	0.13	152.31	0.14	156.45	0.10	159.98	1.00	162.87	0.14	165.63	0.22
0.200	146.92	0.11	150.64	0.13	155.07	0.10	158.69	0.10	161.75	0.14	164.62	0.19
0.250	144.22	0.80	149.02	0.13	153.34	0.09	157.49	0.10	160.65	0.14	163.48	0.18
0.297			147.69	0.10	152.09	0.13	155.80	0.09	159.37	0.25	162.38	0.14
0.350			145.16	0.50	150.75	0.10	154.60	0.09	157.93	0.33	161.38	0.16
0.400			143.71	0.41	148.58	0.10	153.47	0.10	156.23	0.39	160.39	0.14

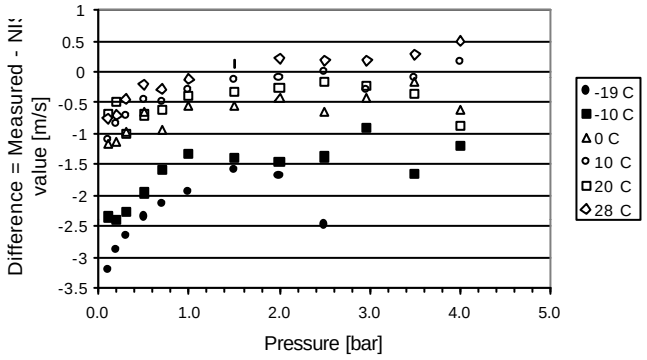

Fig. 3. Differences between measured and predicted values of the velocity of sound in R404A

[7] Mfr.: Prochimac, Neuchatel, Switzerland, 99% purity

Similar comparisons were made in the case of C_4F_{10}[8]. A provisional data file had been added to the NIST REFPROP package for this fluid. Our measurements for the superheated region are shown in Table 4 and differ by an average relative error of ~ -0.2% from the extended NIST predictions at temperatures above 0°C, and by ~ -1.2% for data below -10°C.

Table 4
Velocity of Sound in C_4F_{10}

	Temperature											
	-17.9		-10.0		-0.1		10.0		20.0		30.0	
P_{abs}	SOS	STDV	SOS	STDV	SOS	STDV	SOS	STDV	SOS	STDV	SOS	STDV
[MPa]	[ms^{-1}]	[-]	[ms^{-1}]	[-]	[ms^{-1}]	[-]	[ms^{-1}]	[-]	[ms^{-1}]	[-]	[ms^{-1}]	[-]
0.010	95.10	0.06	96.57	0.07	99.26	0.05	101.05	0.08	103.02	0.10	104.78	0.10
0.020	94.56	0.04	96.22	0.04	98.71	0.05	100.64	0.07	102.70	0.08	104.57	0.08
0.030	93.98	0.04	95.70	0.05	98.33	0.04	100.23	0.06	102.37	0.10	104.25	0.07
0.050			94.78	0.04	97.39	0.04	99.38	0.06	101.71	0.12	103.35	0.12
0.070					96.39	0.07	98.40	0.05	100.86	0.05	103.06	0.05
0.100					94.79	0.10	97.04	0.05	99.66	0.05	103.05	0.08
0.150							95.08	0.05	97.68	0.05	99.91	0.05
0.200									95.63	0.05	98.41	0.07
0.250											96.50	0.05
0.300											94.89	0.05

Tests are continuing with C_3F_8[9] and custom mixtures of C_4F_{10} and C_3F_8. Comparison data will be included in a forthcoming publication.

3.3. Thermal Measurement Data – Heat Transfer Coefficients (HTC)

Typical HTCs for the different fluids measured in the 1.6m "ladder" of Section 2.3 at a dissipation of 8 Watts/block (96 Watts total) are shown in Fig. 4. Values varied in the range $(2 – 5).10^3$ $Wm^{-2}K^{-1}$ depending on the fluid. The highest HTCs were seen in the case of C_3F_8, and the lowest with 50/50 C_4F_{10}/C_3F_8.

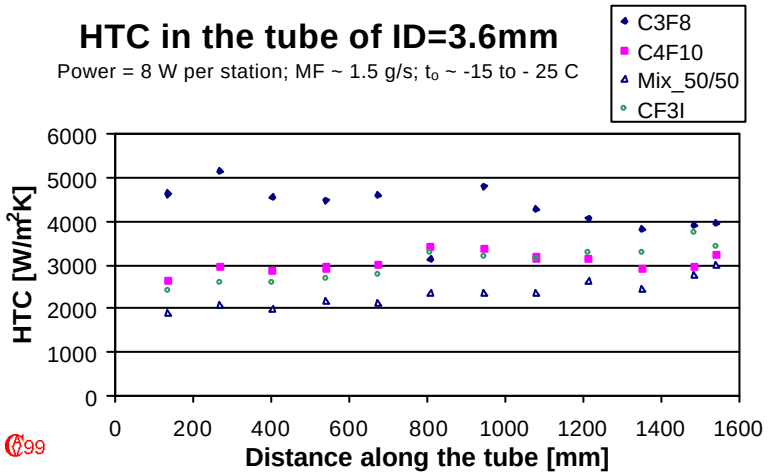

Fig. 4. Heat Transfer Coefficients in a 3.6mm ID tube: C_4F_{10}, CF_3I, C_3F_8 and 50%C_4F_{10}/50% C_3F_8 mixture at similar power and flow rate.

[8] Mfr.: 3-M Corp. Specialty Chemicals Division, St. Paul, MN, USA PFG 5040, grade >99% purity
[9] Mfr: 3-M Corp. Specialty Chemicals Division, St. Paul, MN, USA PFG 5030, grade >99% purity

Heat transfer coefficients were also measured as a function of C_4F_{10}/C_3F_8 relative concentration (Fig. 5), and were found to increase as the mixture became richer in one or other of the components. Similar effects in mixtures have been reported elsewhere [6].

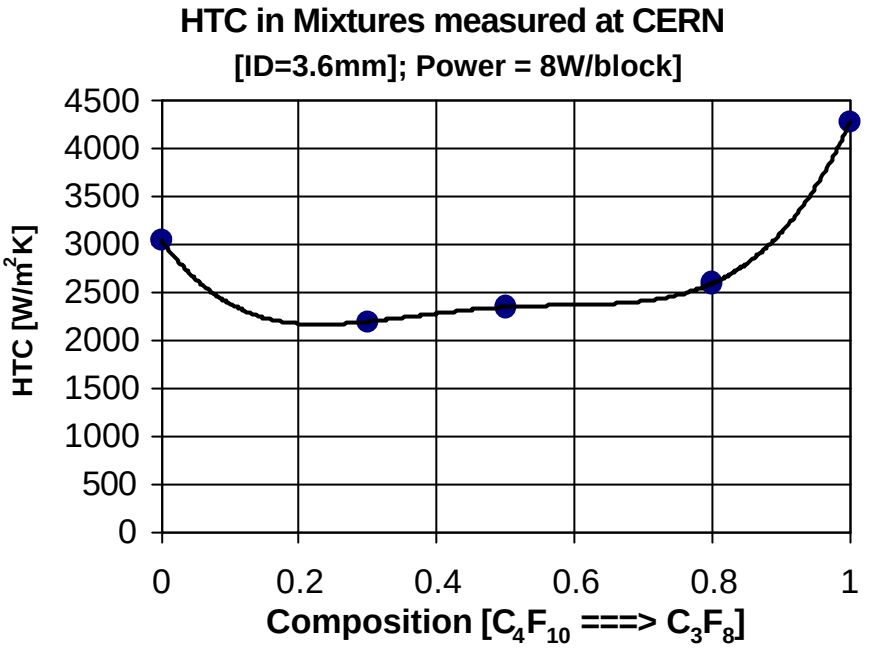

Fig. 5. Measured variation of the Heat Transfer Coefficient in a 3.6mm ID tube with changing C_4F_{10}/C_3F_8 mixture composition.

3.4. Refrigerant Irradiation Studies

3.4.1. Neutron Irradiation

Small (<10 cm^3), static liquid samples of perfluoro-n-hexane (C_6F_{14})[10], CF_3I[11], solid Teflon and iodine (I_2) were irradiated up to 3.10^{13} fast neutrons.cm^{-2} to simulate the expected environment at LHC. Studies showed the main longest-lived radioisotopes to be ^{18}F (106 min: 511 KeV γ emitter) and ^{128}I (25 min: 433 KeV γ emitter). From neutron capture cross section data, the expected activity levels for these radionuclides are in the range 10^4-10^5 Bq.g^{-1} during circulation (for an instantaneous rate ~ 10^6 neutrons.$cm^{-2}s^{-1}$), which is believed to be acceptable in a closed circuit system. However, the overall *measured* level of I_2 activation was considered too high to allow the use of CF_3I in our application.

3.4.2. Radiation-Induced Chemical Modifications

Small (<10 cm^3), static liquid samples of C_6F_{14} and CF_3I were exposed to ^{60}C gamma irradiation. After an absorbed dose of 3 MRad, about 1% by weight of C_6F_{14} liquid had been

[10] Mfr.: 3-M Corp. Specialty Chemicals Division, St. Paul, MN, USA PFG 5060 grade >99%purity
[11] Mfr.: Ajay North America Inc. Powder Springs, GA, 30127-0127, USA

chemically modified: there was chemical evidence of the production of reactive HF, due to impurities containing C-H groups. Scanning electron microscopy and Auger electron spectroscopy were used to characterize the morphologies and elemental compositions of C-, F- and O-containing polymeric deposits formed on stainless steel and aluminum samples immersed in liquid during irradiation. After 6 MRad, surfaces were almost uniformly covered with a polymeric layer of ~ 0.4 μm. Degradation and plate-out were greater in a sample of C_6F_{14} to which 3% (vol.) n-heptane had been added to act as a H-source and simulate the hydrogen containing impurities.

Since saturated fluorocarbons ($C_nF_{(2n+2)}$), are synthesized from alkane precursors, batch testing for residual H contamination (using the characteristic Fourier Transform Infra-Red signature of C-H bonds) is advisable. Techniques for the catalytic removal of $C_nF_{(2n+2-x)}H_x$ contamination have been developed at CERN [11], and could be used in the present application.

After irradiation to 2 MRad, liquid CF_3I had become opaque and breakdown of CF_3I into I_2 and HI was seen. This was not a complete surprise, since CF_3I is a refrigerant with a short (~24 hr) atmospheric half-life. Oily residues (pre-polymers) were observed after the evaporation of the irradiated CF_3I, and thick deposits, including crystalline I_2 were observed on aluminum and stainless steel immersion samples. Although it was possible to clean the CF_3I to remove I_2 and re-establish the transparency, CF_3I was finally abandoned as a coolant owing to its chemical agressivity, even in the un-irradiated state, to elastomer seal materials and also to its high radioactivation in neutron fields.

4. Conclusions

Evaporative cooling has been demonstrated at the full power dissipation of the ATLAS SCT and pixel detectors. Studies with engineering prototypes and measurements of heat transfer coefficient indicate that C_3F_8 is presently the best candidate refrigerant. The low boiling pressure of C_4F_{10} (~350 mbar $_{abs}$ at ~ –25ºC) allows a small pressure head to drive vapor back to the compressor input. Of the fluids with "optimum" thermodynamics (i.e. a saturated vapor pressure ~ 1 bar_{abs} at ~ –25ºC), C_3F_8/C_4F_{10} custom mixtures are less favored due to lower heat transfer coefficient.

Sound velocity measurements made in light gases and xenon compared well with ideal gas predictions. Comparisons with calculations from the NIST package in the low pressure superheated region for R404A and C_4F_{10} also showed good agreement, to better than 0.3% above 0°C region, and to ~ -1.3% for data below -10°C.

Irradiation results suggest that perfluorocarbons (fully fluorinated saturated alcanaes) should be useable in our application. However, CF_3I was rejected due to its poor chemical stability under ionizing radiation, and radioactivation concerns.

5. List of symbols

v_t theoretical (ideal gas) sound velocity (ms^{-1})
P pressure (MPa, bar)
R universal gas constant (8.314 J mol^{-1} K^{-1})
ID inner diameter (mm)

MF mass flow [gs^{-1}]
SOS measured velocity of sound [ms^{-1}]
T temperature (K)
t temperature (C)
m molar mass (kg)

Greek letters
k ratio of specific heats

Subscripts
abs absolute (pressure)
SV saturated vapor
SL saturated liquid

Units
Bq radioactive decays per second

Acknowledgments

The authors thank S. Berry, P. Bonneau, M. Bosteels and P. Ferraudet (CERN) for their help in fabricating the evaporative fluorocarbon recirculators, and J. Thadome (Univ. Wuppertal, Germany) for his help in fabricating the sonar gas analyzer. The research was partly supported by grant No.: CEZ:J04/98:212200008.

References:

[1] ATLAS Pixel Detector Technical Design Report CERN/LHCC/98-13, 31 May 1998
[2] ATLAS Inner Detector Technical Design Report CERN/LHCC/97-16/17, April 1997
[3] G. Hallewell, G. Lenzen, J. Thadome, V. Vacek et al: Progress in Fluorocarbon Evaporative Cooling, ATLAS Pixel Mechanics Meeting, and also ATLAS Review of Cooling System, CERN September 1997
[4] NIST Thermodynamic and Transport Properties of Refrigerants and Refrigerant Mixtures – REFPROP PACKAGE [with extensions], Version 6.01, NIST Gaithersburg, 1998
[5] M.Lísal, V.Vacek: Direct evaluation of vapour-liquid equilibria of mixtures by molecular dynamics using Gibbs-Duhem integration, Molecular Simulation, 18: (1996), 75
[6] M. Lísal, R. Budinský, V. Vacek:"Vapour-liquid Equilibria for Dipolar Two-Centre Lennard-Jones Fluids by Gibbs-Duhem Integration" Fluid Phase Equilibria, 135 (1997),193
[7] G. Hallewell et al: "A sonar based technique for the ratiometric determination of binary gas mixtures", Nucl.Instr. & Meth. A264, (1988), 219.
[8] E. Anderssen, G. Hallewell, V. Vacek, et al: "Fluorocarbon Evaporative Cooling Developments for the ATLAS Pixel and Semiconductor Tracking Detectors", Proc. Fifth Workshop on Electronics for LHC Experiments, Snowmass Co. USA, (September, 1999); also at CERN 99-09 CERN/LHCC99-33, October 1999.
[9] T. Inoue, N. Kawae, M. Monde: Characteristics of Heat Transfer Coefficient During Nucleate Pool Boiling of Binary Mixtures" , Heat & Mass Transfer 33 (1998), 337
[10] S. Ilie, G. Lenzen: "Perfluorocarbon Liquid: Specific Chemical Aspects for use within the DELPHI Ring Imaging Cerenkov Detector" , DELPHI 93-33 RICH54, CERN, 1993.